



## Magnetizable stent-grafts enable endothelial cell capture



Brandon J. Tefft<sup>a</sup>, Susheil Uthamaraj<sup>b</sup>, J. Jonathan Harburn<sup>c</sup>, Ota Hlinomaz<sup>d</sup>, Amir Lerman<sup>a</sup>, Dan Dragomir-Daescu<sup>e</sup>, Gurpreet S. Sandhu<sup>a,\*</sup>

<sup>a</sup> Department of Cardiovascular Diseases, Mayo Clinic, Rochester, MN, USA

<sup>b</sup> Division of Engineering, Mayo Clinic, Rochester, MN, USA

<sup>c</sup> School of Medicine, Pharmacy and Health, Durham University, Stockton-on-Tees, UK

<sup>d</sup> Department of Cardioangiiology, St. Anne's University Hospital, Brno, Czechia

<sup>e</sup> Department of Physiology and Biomedical Engineering, Mayo Clinic, Rochester, MN, USA

### ARTICLE INFO

**Keywords:**

SPION  
Electrospinning  
Polyurethane  
Endothelialization  
BOEC

### ABSTRACT

Emerging nanotechnologies have enabled the use of magnetic forces to guide the movement of magnetically-labeled cells, drugs, and other therapeutic agents. Endothelial cells labeled with superparamagnetic iron oxide nanoparticles (SPION) have previously been captured on the surface of magnetizable 2205 duplex stainless steel stents in a porcine coronary implantation model. Recently, we have coated these stents with electrospun polyurethane nanofibers to fabricate prototype stent-grafts. Facilitated endothelialization may help improve the healing of arteries treated with stent-grafts, reduce the risk of thrombosis and restenosis, and enable small-caliber applications. When placed in a SPION-labeled endothelial cell suspension in the presence of an external magnetic field, magnetized stent-grafts successfully captured cells to the surface regions adjacent to the stent struts. Implantation within the coronary circulation of pigs ( $n=13$ ) followed immediately by SPION-labeled autologous endothelial cell delivery resulted in widely patent devices with a thin, uniform neointima and no signs of thrombosis or inflammation at 7 days. Furthermore, the magnetized stent-grafts successfully captured and retained SPION-labeled endothelial cells to select regions adjacent to stent struts and between stent struts, whereas the non-magnetized control stent-grafts did not. Early results with these prototype devices are encouraging and further refinements will be necessary in order to achieve more uniform cell capture and complete endothelialization. Once optimized, this approach may lead to more rapid and complete healing of vascular stent-grafts with a concomitant improvement in long-term device performance.

### 1. Introduction

Stent-grafts, also known as covered stents, are endovascular devices that can be implanted within a blood vessel using a minimally invasive procedure to create an artificial conduit for blood flow [1]. Common indications for stent-grafts include aortic coarctation, aneurysm, arteriovenous fistula, vein graft degeneration, dissection, perforation, traumatic injury, and hemodialysis access. The synthetic materials present on the blood contacting surface of these devices stimulate thrombosis and neointimal hyperplasia, both of which reduce device patency over time [2,3]. This is especially problematic in small-caliber applications and stent-grafts are therefore currently limited to routine use in medium- and large-caliber applications.

An effective strategy for improving performance in large- and medium-caliber applications and enabling small-caliber applications is to rapidly heal the stent-graft by establishing a confluent and robust endothelium on the blood contacting surface [1]. Endothelial cells

serve as a natural barrier between circulating blood elements and underlying tissues and inhibit both thrombosis and neointimal hyperplasia. A variety of approaches for coating the blood contacting surface of implantable devices with endothelial cells have been studied [4]; however, poor cell retention upon exposure to the shear stress of circulating blood remains problematic [5].

Our group has developed an approach to rapidly and stably target endothelial cells to implantable devices using magnetic forces. We have developed a process for synthesizing superparamagnetic iron oxide nanoparticles (SPION) and using them to label blood outgrowth endothelial cells (BOEC) [6]. Furthermore, we have demonstrated that SPION-labeled BOECs can be targeted to magnetic devices including vascular grafts [7] and stents [8–10]. In this study, we extend our magnetic cell targeting approach to a novel ferromagnetic stent-graft design and demonstrate successful cell capture and retention after 7 days of implantation in porcine coronary circulation.

\* Corresponding author.

E-mail address: [sandhu.gurpreet@mayo.edu](mailto:sandhu.gurpreet@mayo.edu) (G.S. Sandhu).

## 2. Methods and materials

### 2.1. SPION synthesis

SPIONs were synthesized by coating magnetite ( $\text{Fe}_3\text{O}_4$ ) with poly(lactic-co-glycolic acid) (PLGA) as previously described [6]. Briefly, magnetite nanoparticles approximately 10 nm in diameter were synthesized by stirring an aqueous solution of iron(II) chloride tetrahydrate and iron(III) chloride at 1000 RPM and 50 °C. The magnetite nanoparticles were then precipitated using ammonium hydroxide, coated with oleic acid to form a gel, and purified. Next, the magnetite nanoparticles were coated with a shell of PLGA approximately 50 nm thick by high speed oil-in-water emulsification (1:15 ratio of magnetite to PLGA by mass) using Pluronic F-127 as a stabilizer. Finally, the PLGA-magnetite SPIONs were washed and lyophilized prior to storage at -20 °C.

### 2.2. BOEC culture

BOECs were generated from porcine peripheral blood mononuclear cells as previously described [11]. Briefly, 50–200 mL of peripheral blood was collected from an anesthetized pig and immediately mixed with approximately 10 units/mL of heparin to prevent coagulation. The heparinized blood was diluted 1:1 with phosphate buffered saline (PBS) and the mononuclear cell fraction was isolated by density gradient centrifugation (Histopaque 1077, GE Healthcare Life Sciences, Piscataway, NJ). The mononuclear cells were washed and residual erythrocytes were lysed using a 0.6% ammonium chloride solution. Next, the mononuclear cells were washed twice more and cultured in fibronectin-coated wells with EGM-2 cell culture medium (Lonza, Basel, Switzerland). BOEC colonies typically formed within 10–14 days and millions of highly proliferative and phenotypically homogenous BOECs were typically generated within 2–3 weeks. Our group has previously characterized these cells when derived from human [11] and pig [7] blood including positive expression of von Willebrand factor and lectin uptake, which are indicative of endothelial cell phenotype.

BOECs in passages 1–2 were used for experiments. One day prior to use, BOECs were labeled with SPIONs by adding to cell culture medium at a concentration of 200 µg/mL and incubating overnight at 37 °C as previously described [6]. BOECs endocytose the SPION particles and store them within cytoplasmic endosomes as we have shown previously [9]. Just prior to use, BOECs were stained with a fluorescent marker (CM-Dil, ThermoFisher Scientific, Waltham, MA) by incubating at a concentration of 5 µL/mL in cell culture medium for 30 min at 37 °C.

### 2.3. Stent-graft fabrication

Stent-grafts were fabricated by coating stents made from magnetic 2205 duplex stainless steel (2205 SS) or non-magnetic 316L stainless steel (316L SS) [12] with electrospun polyurethane nanofibers as previously described [13]. Briefly, a 15% polyurethane in dimethylacetamide (DMA) solution (DSM Biomedical, Exton, PA) was loaded into a 5 mL glass syringe and a blunt needle was attached. A syringe pump was used to extrude the polyurethane solution at a rate of 0.01 mL/min while a power supply was used to provide 20 kV of potential to the blunt needle. A 3 mm diameter stainless steel mandrel coated with a food-grade support material (EnvisionTEC, Dearborn, MI) was placed 20 cm from the blunt needle, grounded, and rotated at 50 RPM. After 2 h of nanofiber collection on the rotating mandrel, a stent was crimped onto the mandrel, and nanofibers were collected for a further 3 h. After trimming the excess polyurethane, dissolving the support material in water, and removing from the mandrel, the resulting stent-graft consisted of a stent sandwiched between a 100 µm thick inner layer and a 150 µm thick outer layer of polyur-

ethane nanofibers. Stent-grafts were carefully inspected prior to sterilization with ethylene oxide gas.

### 2.4. In vitro cell capture studies

SPION-labeled BOECs were suspended in PBS at a concentration of  $1 \times 10^6$  cells/mL. Fluorescence microscopy was used to visualize the capture of cells as the cell suspension was pipetted over a magnetized stent-graft in the presence of an external magnetic field. The external magnetic field was generated by two 1.0 T rare earth magnets positioned on opposite sides of the device with opposing poles facing inward. One magnet was placed 8 cm above the device and the other was placed 19 cm below at an angle of 45° from the vertical to simulate the positioning of the magnets during animal implantation studies.

### 2.5. Porcine implantation studies

All animal procedures were performed in accordance with Mayo Clinic Institutional Animal Care and Use Committee (IACUC) policy. Domestic Yorkshire pigs (n=13) weighing 40–50 kg were anesthetized using an intramuscular injection of 2–3 mg/kg Xylazine, 5 mg/kg Telazol, and 0.05 mg/kg atropine. Continuous inhalation of 1.2–1.5% isoflurane was used to maintain anesthesia during the procedure. Carotid access was used to cannulate the right or left coronary artery with a 9F guide catheter. A stent-graft sterilized by ethylene oxide gas was crimped onto an over-the-wire balloon catheter and deployed within a segment of the right coronary artery or the circumflex artery. Each pig received 1–2 stent-grafts for a total of n=14 magnetic 2205 SS stent-grafts and n=10 non-magnetic 316L SS stent-grafts. Approximately  $2-4 \times 10^6$  autologous BOECs labeled with SPIONs were delivered to the implanted 2205 SS stent-grafts using the balloon catheter over a period of 4 min of blood flow occlusion. The number of delivered cells is approximately an order of magnitude larger than the  $2.8 \times 10^5$  cells needed to completely cover the inner surface of the stent-graft at an optimal seeding density of  $2 \times 10^5$  cells/cm<sup>2</sup> [14].

An external magnetic field was applied to the stent-graft during cell delivery and for 1–2 h afterwards by strapping one 1.0 T rare earth magnet above the sternum and another on the right lateral side of the chest wall with opposing poles facing inward. Using magnetic field measurements of an in vitro phantom, we estimated this arrangement of magnets provided a uniform magnetic field of approximately 120 G at the location of the implant. With the stent-graft at that location, the magnetic field remained approximately 120 G but local field gradients allowed for generation of magnetic force. The magnets were left strapped to the pigs as long as possible in order to maximize cell retention, but they were promptly removed once the pigs exhibited sternal recumbency and semi-consciousness due to animal safety considerations. Pigs were allowed to recover and were administered 75 mg clopidogrel and 325 mg aspirin daily beginning 3 days prior to the procedure and continuing until sacrifice.

Pigs were sacrificed after 7 days and the treated arteries were carefully dissected, cleaned, and fixed in 10% formalin solution. Selected samples were sectioned longitudinally, splayed open, and assessed using light microscopy, fluorescence microscopy, and scanning electron microscopy (SEM). Remaining samples were analyzed histologically by embedding in plastic, cross-sectioning, and staining with H & E, Movat's pentachrome, or Prussian blue for iron according to established protocols [15] (CVPath Institute, Gaithersburg, MD).

## 3. Results

When delivered to a 2205 SS stent-graft in the presence of an external magnetic field in vitro, SPION-labeled BOECs were captured to the polyurethane cover at regions adjacent to underlying stent struts (Fig. 1). Cell capture was not evident at the regions between stent struts. This confirmed that the 100–150 µm thick polyurethane cover

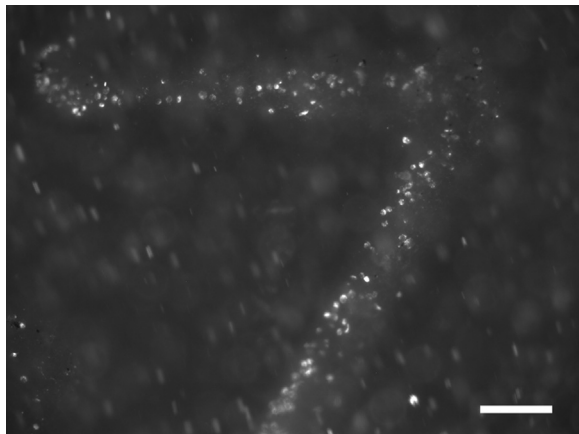


**Fig. 1.** Fluorescence micrograph of a magnetic 2205 SS stent-graft capturing SPION-labeled BOECs (white) to the surface regions adjacent to underlying stent struts during an in vitro experiment. Scale bar=200  $\mu$ m.

does not interfere with the ability of the underlying 2205 SS stent to capture SPION-labeled BOECs.

The stent-grafts were successfully implanted using standard cardiac catheterization techniques. The stent-grafts crimped onto the balloon catheter without obvious damage to the stainless steel stents or the polyurethane cover. Of the 13 pigs studied, 12 recovered from the procedure and survived to the designed study endpoint of 7 days without complication and 1 died shortly after the procedure likely as a result of complications that arose during the carotid cut-down. Upon gross visual examination at explant, the hearts appeared normal with no signs of infarction. The stent-grafts were all widely patent with no evidence of thrombosis or unusual inflammation (Fig. 2A). The stent-grafts also displayed uniformly expanded struts without signs of fracture, indicating successful deployment within the vessels. Additionally, the stent-grafts displayed intact polyurethane covers, indicating they did not tear or rupture during crimping and expansion. Delamination of the inner and outer polyurethane layers was also not observed.

A thin and uniform neointima formed on the inner surface of all stent-grafts (Fig. 2B). This neotissue was translucent, shiny, and overall similar in appearance to the native vessel wall. A uniform cell layer was observed on the luminal surface of the neointima in select regions,

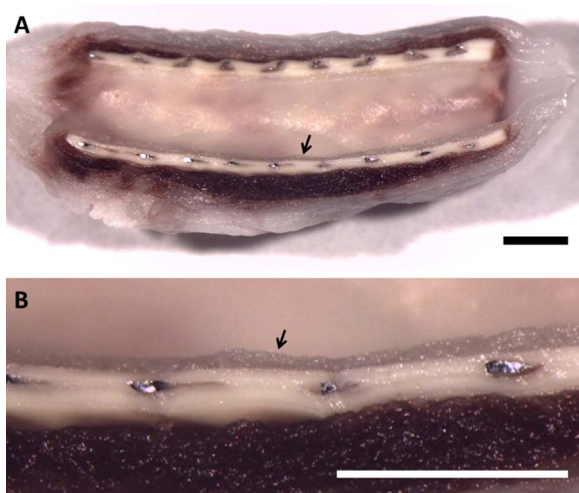


**Fig. 2.** Photographs of stent-grafts explanted after 7 days in porcine coronary circulation, sectioned longitudinally, and splayed open to reveal the luminal surface. (A) Stent-grafts are widely patent and completely covered by a neointima (black arrow). (B) The neointima is thin and uniform on the luminal surface of the stent-graft (black arrow). Scale bars=2 mm.

usually near the ends of the stent-graft (Fig. 3A). This cell layer was typically observed to be continuous with that of the neighboring native vessel (Fig. 3B). The middle regions of the stent-grafts were generally not well covered by cells, leaving the neointima exposed.

Histological analysis of cross-sections confirmed patency and lack of thrombosis and inflammation (Fig. 4A). Uniformly expanded struts and intact polyurethane covers were also confirmed. The thin and uniform neointima (approximately 100  $\mu$ m thick) was observed to cover the entire circumference of the inner surface of all stent-grafts. Iron staining demonstrated capture and retention of SPION-labeled cells in select regions adjacent to stent struts (Fig. 4B) and between stent struts (Fig. 4C) for 2205 SS stent-grafts only.

Fluorescence microscopy revealed capture and retention of fluorescently-labeled BOECs in select regions of magnetic 2205 SS stent-grafts (Fig. 5B), whereas non-magnetic 316L SS stent-grafts contained virtually none (Fig. 5A). The majority of fluorescently-labeled cells were observed in the neointima adjacent to stent struts; however, they were also observed in the neointima between stent struts. Where present, fluorescently-labeled cells generally appeared throughout the thickness of the neointima.

#### 4. Discussion

A stent-graft capable of rapid healing will be less susceptible to thrombosis and neointimal hyperplasia and will therefore achieve superior patency rates and clinical outcomes, especially in small-caliber applications. The ferromagnetic stent-graft studied in this report is the first of its kind and enables a variety of magnetic targeting applications including cell, drug, and gene delivery. Our group and others have previously demonstrated the benefits of delivering cells [9,10,16,17], drugs [18–21], and genes [22] to magnetized stents as well as cells to injured vessels [23,24]. Stent-grafts have distinct indications from those of stents, such as repair of weakened or damaged vessels, and a magnetic stent-graft allows additional patient populations to benefit from the magnetic targeting approach.

Commercial stents are typically made from austenitic stainless steel grades including 304 and 316L. The magnetic cell capture approach studied in this report required using our previously developed stents made from 2205 grade stainless steel, which has ferromagnetic properties due to its duplex austenite/ferrite microstructure [10]. Compared to the austenitic stainless steel grades, the 2205 grade exhibits approximately 25% higher ultimate tensile strength, 135% higher yield strength, 60% lower ultimate tensile strain, and superior corrosion resistance [25,26]. The 2205 grade is also somewhat more difficult to machine, but high quality stents can be manufactured using standard tube drilling and grinding followed by laser cutting of the strut pattern [12].

Adding a polymer cover to a stent to create a stent-graft introduces new failure modes and increases the difficulty of device delivery. The cover must be strong enough to withstand the crimping and expansion process without tearing, delaminating, or detaching from the stent. It must also be thin enough to allow for crimping to a low profile as well as flexing through the vasculature to the delivery site. An appropriate balance between strength and deliverability was achieved with an inner layer thickness of 100  $\mu$ m and an outer layer thickness of 150  $\mu$ m for a total cover thickness of 250  $\mu$ m [13]. While this adds considerable bulk to the 90  $\mu$ m thick stent struts, the elasticity of polyurethane allowed the devices to crimp into a 9F guide catheter for delivery to the coronary circulation without noticeable damage to the devices.

Overall, the stent-grafts handled well and could be implanted into the porcine coronary circulation using standard techniques. The devices remained fully and uniformly expanded during 7 days of implantation. They also maintained patency and did not display any acute thrombosis or inflammation. Healing at 7 days consisted of a thin and uniform neointima with partial cell coverage. Since migration of cells through the polyurethane cover is not possible, this neointima

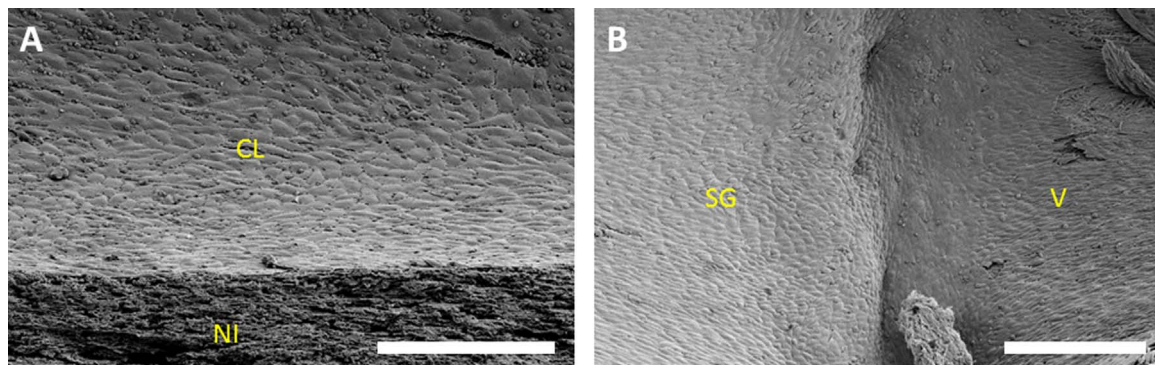


**Fig. 3.** Scanning electron micrographs of the luminal surface of stent-grafts explanted after 7 days in porcine coronary circulation, sectioned longitudinally, and splayed open. (A) A confluent cell layer covering the neointima. (B) A continuous cell layer covering the stent-graft and the neighboring native vessel. CL=cell layer, NI=neointima, SG=stent-graft, and V=vessel. Scale bars=200  $\mu$ m.

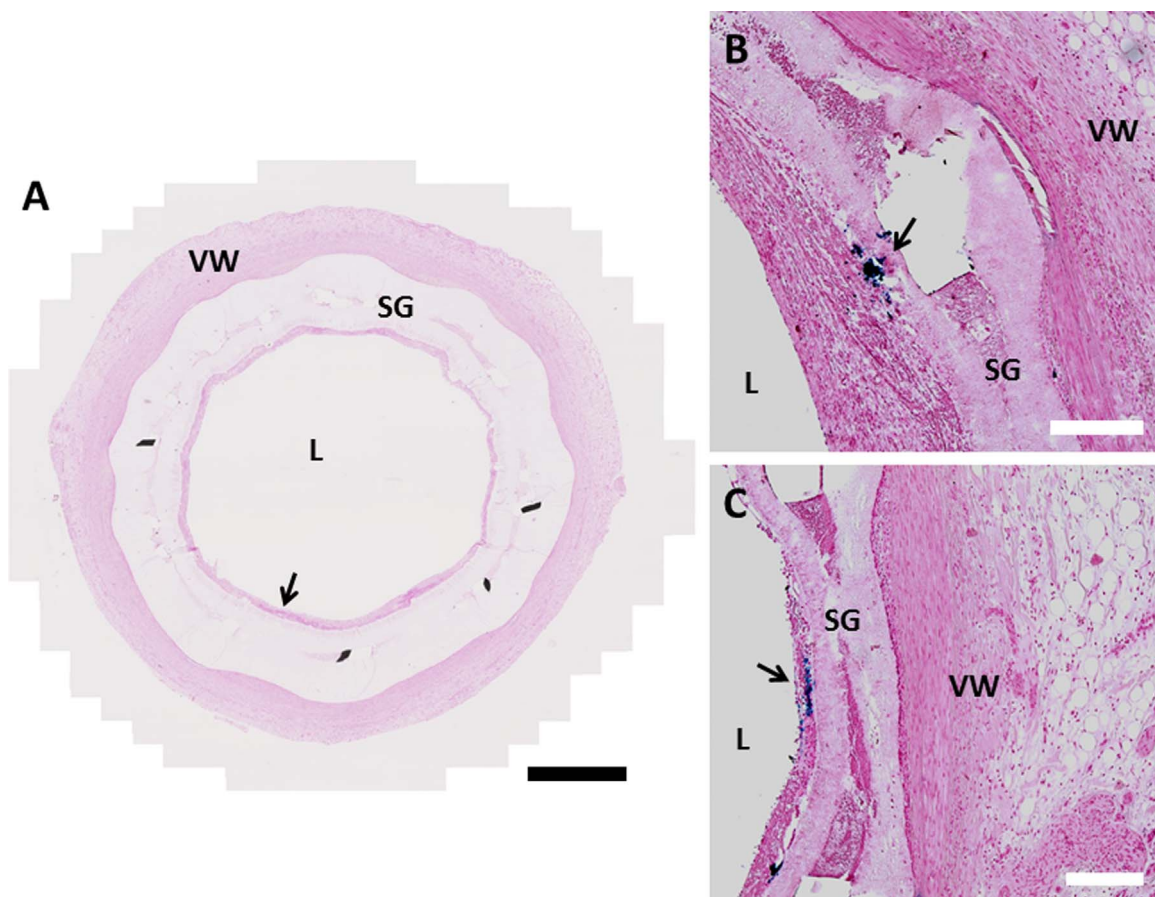


**Fig. 4.** Histology of stent-grafts explanted after 7 days in porcine coronary circulation and cross-sectioned. (A) A widely patent stent-graft with a thin and uniform neointima on the luminal surface (black arrow). (B) SPION-labeled cells (blue) captured to the luminal surface adjacent to a stent strut (black arrow). (C) SPION-labeled cells (blue) captured to the luminal surface between stent struts (black arrow). L=lumen, SG=stent-graft, and VW=vessel wall. Scale bar in (A)=1 mm and scale bars in (B) and (C)=200  $\mu$ m. (For interpretation of color in this figure legend, the reader is referred to the web version of this article.)

likely consisted of a mixture of smooth muscle cells that migrated from the neighboring native vessel, delivered BOECs, and circulating blood elements including endothelial progenitor cells, monocytes, platelets, and fibrin. Similar cell coverage on the surface of the neointima was observed for both 2205 SS stent-grafts and 316L SS stent-grafts and was most prominent near the ends of the stent-grafts, indicating the origin of these cells is likely migration from the neighboring native vessel. The cobblestone morphology of these cells is consistent with an endothelium; however, the samples were not analyzed for endothelial cell markers in this study.

Although successful endothelial cell capture and retention were

observed for 2205 SS stent-grafts, capture was not uniform and did not result in noticeably superior healing for magnetic 2205 SS stent-grafts when compared with non-magnetic 316L SS stent-grafts. In vitro studies indicated that cell capture is limited to regions adjacent to underlying stent struts. Since the stent struts are approximately 1.5 mm apart, cells must proliferate and migrate over a distance of approximately 750  $\mu$ m in order to cover the entire luminal surface. Such a short distance is reasonable for highly proliferative BOECs to cover, but irreversible adverse reactions may begin at the surface before the cells arrive. While delivered cells were observed to migrate between struts and were incorporated into the neointima in select regions, their

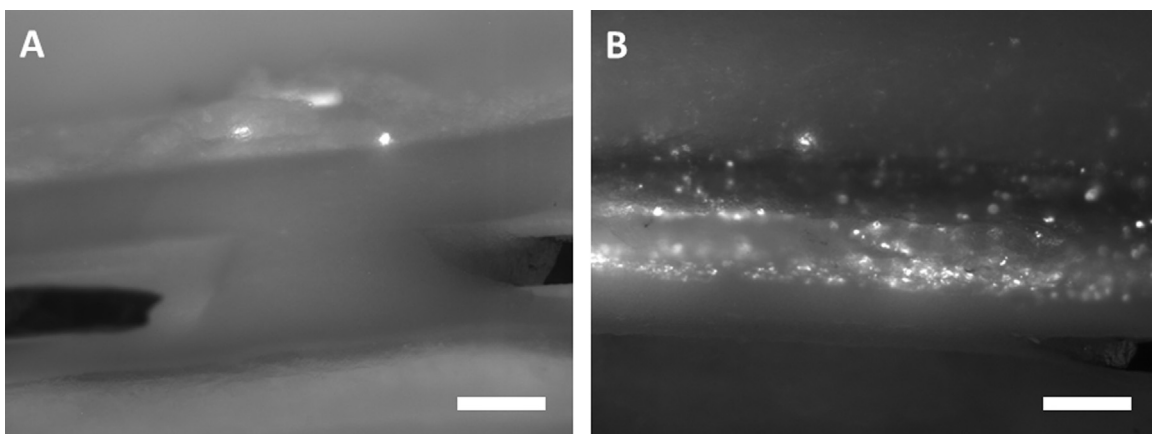


**Fig. 5.** Fluorescence micrographs of stent-grafts explanted after 7 days in porcine coronary circulation, sectioned longitudinally, and splayed open. (A) Very few SPION-labeled BOECs (white) are captured to the luminal surface of non-magnetic 316L SS stent-grafts. (B) Numerous SPION-labeled BOECs (white) are captured to the luminal surface of magnetic 2205 SS stent-grafts. Scale bars=200  $\mu$ m.

coverage on the surface of the neointima was limited. This indicates that cell migration did not occur quickly enough and the incompletely healed neointima is expected to continue thickening with time.

While the initial healing response at 7 days was encouraging, more uniform endothelial cell capture immediately following implantation is likely needed in order to achieve a complete and stable healing response. This may be achieved by incorporating magnetic 2205 SS powder into the polyurethane nanofiber cover in order to target cells to the entire surface rather than to only the regions adjacent to magnetic stent struts.

## 5. Conclusion

The ferromagnetic stent-graft design exhibited suitable mechanical properties for transcatheter delivery to a coronary artery using standard cardiac catheterization techniques. The struts expanded uniformly and the stent-grafts did not show any signs of material failure or damage. Healing at 7 days was encouraging as evidenced by a thin and uniform neointima and lack of thrombosis and inflammation. Magnetically targeted cells were successfully captured and retained during 7 days of implantation in the coronary circulation. Although delivered endothelial cells were found on the luminal surface adjacent to stent struts as well as between stent struts, endothelialization was incomplete and more uniform cell delivery is likely necessary to achieve stable long-term healing. Future studies will improve the magnetic properties of the stent-grafts with the goal of achieving uniform cell capture to the entire luminal surface.

## Acknowledgments

The authors would like to acknowledge funding from the European Regional Development Fund – FNUSA-ICRC (no. CZ.1.05/1.1.00/02.0123), the American Heart Association Scientist Development Grant (AHA #06-35185N), and the National Institutes of Health (NIH #T32HL007111, #K99HL129068).

## References

- [1] Z. Sun, Endovascular stents and stent grafts in the treatment of cardiovascular disease, *J. Biomed. Nanotechnol.* 10 (2014) 2424–2463.
- [2] M. Takano, M. Yamamoto, T. Inami, D. Murakami, Y. Seino, K. Mizuno, Delayed healing of a coronary stent graft, *JACC Cardiovasc. Interv.* 4 (2011) 466–467.
- [3] M. Takano, M. Yamamoto, S. Inami, Y. Xie, D. Murakami, K. Okamatsu, T. Ohba, Y. Seino, K. Mizuno, Delayed endothelialization after polytetrafluoroethylene-covered stent implantation for coronary aneurysm, *Circ. J.* 73 (2009) 190–193.
- [4] R.R. Ravindranath, A. Romaschin, M. Thompson, In vitro and in vivo cell-capture strategies using cardiac stent technology – a review, *Clin. Biochem.* 49 (2016) 186–191.
- [5] C. Tresoldi, A.F. Pellegata, S. Mantero, Cells and stimuli in small-caliber blood vessel tissue engineering, *Regen. Med.* 10 (2015) 505–527.
- [6] B.J. Tefft, S. Uthamaraj, J.J. Harburn, M. Klabusay, D. Dragomir-Daescu, G.S. Sandhu, Cell labeling and targeting with superparamagnetic iron oxide nanoparticles, *J. Vis. Exp.* (105) (2015) e53099.
- [7] S.V. Pislaru, A. Harbuzariu, G. Agarwal, T. Witt, R. Gulati, N.P. Sandhu, C. Mueske, M. Kalra, R.D. Simari, G.S. Sandhu, Magnetic forces enable rapid endothelialization of synthetic vascular grafts, *Circulation* 114 (2006) I314–I318.
- [8] S.V. Pislaru, A. Harbuzariu, R. Gulati, T. Witt, N.P. Sandhu, R.D. Simari, G.S. Sandhu, Magnetically targeted endothelial cell localization in stented vessels, *J. Am. Coll. Cardiol.* 48 (2006) 1839–1845.
- [9] B.J. Tefft, J.Y. Gooden, S. Uthamaraj, J.J. Harburn, M. Klabusay, D.R. Holmes, R.D. Simari, D. Dragomir-Daescu, G.S. Sandhu, Magnetizable duplex steel stents enable endothelial cell capture, *IEEE Trans. Magn.* 49 (2013) 463–466.
- [10] S. Uthamaraj, B.J. Tefft, M. Klabusay, O. Hlinomaz, G.S. Sandhu, D. Dragomir-Daescu, Design and validation of a novel ferromagnetic bare metal stent capable of capturing and retaining endothelial cells, *ABME* 42 (2014) 2416–2424.
- [11] R. Gulati, D. Jevremovic, T.E. Peterson, S. Chatterjee, V. Shah, R.G. Vile, R.D. Simari, Diverse origin and function of cells with endothelial phenotype obtained from adult human blood, *Circ. Res.* 93 (2003) 1023–1025.
- [12] S. Uthamaraj, B.J. Tefft, O. Hlinomaz, G.S. Sandhu, D. Dragomir-Daescu, Ferromagnetic bare metal stent for endothelial cell capture and retention, *J. Vis. Exp.* 103 (2015) e53100.
- [13] S. Uthamaraj, B.J. Tefft, S. Jana, O. Hlinomaz, M. Kalra, A. Lerman, D. Dragomir-Daescu, G.S. Sandhu, Fabrication of small caliber stent-grafts using electrospinning and balloon expandable bare metal stents, *J. Vis. Exp.* (2016).
- [14] K.C. Kent, A. Oshima, A.D. Whittemore, Optimal seeding conditions for human endothelial cells, *Ann. Vasc. Surg.* 6 (1992) 258–264.
- [15] E.B. Prophet, *Laboratory Methods in Histotechnology*, Armed Forces Institute of Pathology, American Registry of Pathology, Washington, DC.
- [16] B. Polyak, I. Fishbein, M. Chorny, I. Alferiev, D. Williams, B. Yellen, G. Friedman, R.J. Levy, High field gradient targeting of magnetic nanoparticle-loaded endothelial cells to the surfaces of steel stents, *Proc. Natl. Acad. Sci. USA* 105 (2008) 698–703.
- [17] R.F. Adamo, I. Fishbein, K. Zhang, J. Wen, R.J. Levy, I.S. Alferiev, M. Chorny, Magnetically enhanced cell delivery for accelerating recovery of the endothelium in injured arteries, *J. Control. Release: Off. J. Control. Release Soc.* 222 (2016) 169–175.
- [18] M. Kempe, H. Kempe, I. Snowball, R. Wallen, C.R. Arza, M. Gotberg, T. Olsson, The use of magnetic nanoparticles for implant-assisted magnetic drug targeting in thrombolytic therapy, *Biomaterials* 31 (2010) 9499–9510.
- [19] M. Chorny, I. Fishbein, B.B. Yellen, I.S. Alferiev, M. Bakay, S. Ganta, R. Adamo, M. Amiji, G. Friedman, R.J. Levy, Targeting stents with local delivery of paclitaxel-loaded magnetic nanoparticles using uniform fields, *Proc. Natl. Acad. Sci. USA* 107 (2010) 8346–8351.
- [20] T. Rathel, H. Mannell, J. Pircher, B. Gleich, U. Pohl, F. Krotz, Magnetic stents retain nanoparticle-bound antirestenotic drugs transported by lipid microbubbles, *Pharm. Res.* 29 (2012) 1295–1307.
- [21] M.O. Aviles, H.T. Chen, A.D. Ebner, A.J. Rosengart, M.D. Kaminski, J.A. Ritter, In vitro study of ferromagnetic stents for implant assisted-magnetic drug targeting, *J. Magn. Magn. Mater.* 311 (2007) 306–311.
- [22] M. Chorny, I. Fishbein, J.E. Tengood, R.F. Adamo, I.S. Alferiev, R.J. Levy, Site-specific gene delivery to stented arteries using magnetically guided zinc oleate-based nanoparticles loaded with adenoviral vectors, *FASEB J.* 27 (2013) 2198–2206.
- [23] J. Riegler, A. Liew, S.O. Hynes, D. Ortega, T. O'Brien, R.M. Day, T. Richards, F. Sharif, Q.A. Pankhurst, M.F. Lythgoe, Superparamagnetic iron oxide nanoparticle targeting of MSCs in vascular injury, *Biomaterials* 34 (2013) 1987–1994.
- [24] P.M. Consigny, D.A. Silverberg, N.J. Vitali, Use of endothelial cells containing superparamagnetic microspheres to improve endothelial cell delivery to arterial surfaces after angioplasty, *J. Vasc. Interv. Radiol.* 10 (1999) 155–163.
- [25] W.T. Tsai, M.S. Chen, Stress corrosion cracking behavior of 2205 duplex stainless steel in concentrated NaCl solution, *Corros. Sci.* 42 (2000) 545–559.
- [26] J.A. Platt, A. Guzman, A. Zuccari, D.W. Thornburg, B.F. Rhodes, Y. Oshida, B.K. Moore, Corrosion behavior of 2205 duplex stainless steel, *Am. J. Orthod. Dentofac.* 112 (1997) 69–79.